International Journal of Power and Energy Systems, Vol. 43, No. 10, 2023
An Open Access Paper

NUMERICAL AND EXPERIMENTAL STUDY ON THE EFFECT OF OVERLAP ON SAVONIUS WIND TURBINE

Zaki Alomar,* Gerard Khoury,** Jihad Rishmany,** and Michel Daaboul**

Abstract

Wind as a renewable energy source is not yet fully exploited despite the permanent availability of this source. Moreover, in countries where renewable energy regulations are still absent, large-scale applications are still not available. The only wind turbines implemented are small-scaled applications owed to individual contributions. In this context, the Savonius wind turbine seems to be the most suitable choice at this scale because of its relatively low noise level, ease of manufacturing and maintenance, and self-starting aspect even at low wind speeds. However, the major drawback of such a turbine is its relatively low efficiency. In this framework, this study aims at assessing the various design parameters (number of blades, height-to-diameter ratio, and overlap ratio) of a Savonius wind turbine in an attempt to increase its efficiency. This is realised *via* computational fluid dynamics simulations followed by experimental validation through wind tunnel testing. Results show that the optimum configuration consists of a two-blade S-rotor with around 18% overlap. Future improvements could include shielding the returning blade to increase the torque.

Key Words

CFD, overlap, power generation, Savonius, wind tunnel testing, wind turbine

1. Introduction

1.1 Problem Statement

Wind is a renewable, environmentally clean source of energy poised to take a high portion of the world's energy market during the next few decades. The rapid growth in the wind energy sector expresses itself in the research and investments aimed towards the development of new wind technologies and the optimisation of the current ones. In addition, current trends aim at combining both wind and solar energy resources in hybrid systems with intelligent algorithms [1], [2]. Nevertheless, many countries are still struggling to fully exploit their wind resources either due to the low potential wind areas, lack of regulations, or the wind power plant initial cost. Herein, individual contributions are of particular importance. For instance, a house can be turned into a source of renewable energy by simply adding a wind turbine. Therefore, several attempts have been made to design practical, cost-effective, quiet, and efficient wind turbines ideal for small-scale applications. This would be most beneficial not only for developed countries for raising environmental awareness but also for third world countries deprived from electrical power especially with the lack of state-level initiatives which leaves it only to individual contributions to the sector.

Apart from its relatively low efficiency with respect to horizontal axis wind turbines (HAWTs), the Savonius wind turbine satisfies all the aforementioned criteria. It is relatively easy to build and maintain. In addition to its low noise production which makes it implementable into towns or inner-city environment, it is independent of the wind direction and can operate in turbulent wind conditions with relatively good self-starting capability at low wind speeds. Although the Savonius turbine is well suited for residential applications, the integration of such system is hindered by its low efficiency and power output. For that reason, many studies have been carried out to increase its performance. It was perceived that optimising the various design parameters (*i.e.*, blade size, overlap ratio, endplates, *etc.*) can highly improve the turbine's performance. In this context, the aim of this work is to numerically determine the optimum configuration of the rotor/shield design that is capable of fulfilling the needs of a typical household in low wind-speed areas. Overall, this paper instigated with an extensive state-of-the-art concerning the Savonius turbine followed by the numerical simulations methodology and experimental validation by running wind tunnel testing on small-scale prototypes and concluded with an overall assessment of the different configurations investigated.

* Free University of Bolzano/Bozen, 39100 Bolzano, Italy; e-mail: zalomar@unibz.it
** Department of Mechanical Engineering, University of Balamand, Al Kurah, Lebanon; e-mail: gerard.khoury151@gmail.com; {jihad.rishmany, michel.daaboul}@balamand.edu.lb
Corresponding author: Michel Daaboul

(DOI: 10.2316/J.2023.203-0450)

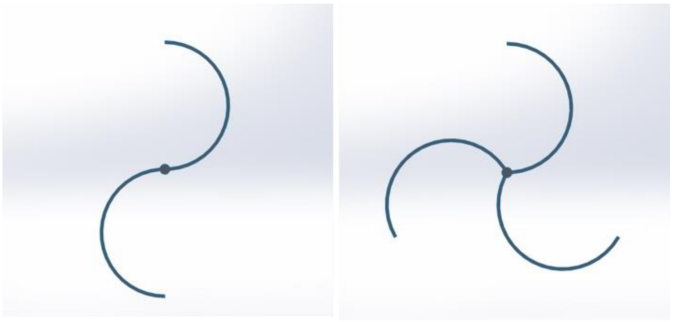

Figure 1. Top view of S-rotor with 2 and 3 blades.

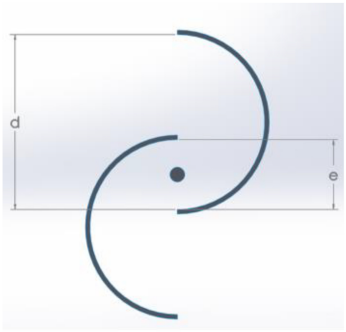

Figure 2. Overlap ratio of the rotor.

1.2 Design Parameters for Savonius Wind Turbine

The conventional Savonius wind turbine, also known as S-rotor, is a drag-type turbine that consists of two semi-circular blades mounted on a vertical shaft. The turbine operates based on the difference in the drag forces between its advancing and returning blade. This difference in drag combined with the side forces are translated into torque [3] and the value of the net torque determines the rotor mechanical power [4]. The maximum power coefficient (C_p) reached by the traditional S-rotor is 0.25 [5]. This power is relatively low, especially if compared with other types of turbines (*i.e.*, Darrieus and HAWT). Therefore, comprehensive studies have been conducted to determine the optimum set of design parameters that maximise the efficiency and power output of the Savonius rotor.

The effect of the number of blades on the performance of the rotor was investigated by several researchers. Sheldahl *et al.* [5], Ali [6], and Saha *et al.* [7] proved experimentally that increasing the number of blades leads to a lower power coefficient (C_p). This is mainly attributed to the fact that for a multi-bladed rotor (Figure 1), the deflected air from one blade exerts a force on the following blade in the opposite direction of rotation resulting in a decrease of the net torque. Hence, a two-bladed system was proven to be the finest configuration.

Another crucial design parameter studied is the overlap ratio (OR). The overlap ratio ($OR = \beta = e/d$) is the ratio of the overlap distance e to the rotor's blade diameter d (Figure 2). Varying the overlap ratio has a significant impact on the overall performance of the turbine due to the change of the flow structure inside the rotor [8]. Previous

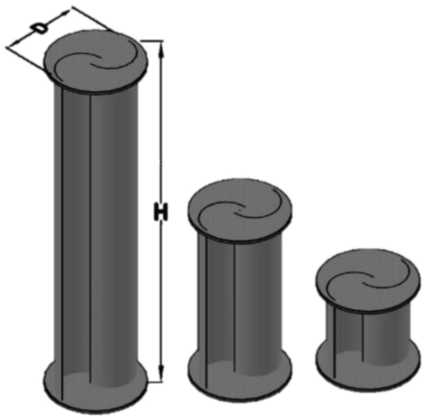

Figure 3. Aspect ratio of the rotor [4]. *Reproduced with permission from Renewable Energy. 12, 99 (2016). Copyright 2016 Elsevier.*

numerical and experimental works, found in the literature, have highlighted the influence of the overlap ratio on the value of the rotor power coefficient. Nonetheless, there is a clear discrepancy in the literature about the overlap optimal value. For instance, Kamoji *et al.* [9] and Fujisawa [10] indicated that an overlap of 0.15 yielded the best performance. Blackwell *et al.* [11] proved experimentally that the optimal value lies within the 0.1–0.15 range. Menet and Bourabaa [12], on the other hand, obtained the highest torque coefficient for an overlap ratio of 0.242. In fact, the overlap optimal value changes with the variation of other design parameters and the operating wind speed. By slightly modifying the blade shape of the conventional Savonius, Kamoji *et al.* [9] found that the rotor performs better without an overlap. Therefore, a parametric study must be carried out to determine the optimal value of the overlap ratio catered to the actual design and the rotor's working conditions.

Other design parameters, such as the aspect ratio and the number of stages, were also considered by many scholars. The aspect ratio ($AR = \alpha = H/D$) is the ratio between the rotor's height H and its diameter D (Figure 3). The aspect ratio should be optimised based on the required output of the turbine. A higher AR leads to a higher RPM but a lower torque and *vice versa* [4]. Generally, a rotor with an aspect ratio neighbouring unity exhibits the best performance [8]. Concerning the number of stages, a multistage rotor produces a more uniform torque along the 360° rotation, though it increases the inertia of the rotor. That extra mass of inertia must be carried by a single stage when the other stages are in the idle angle position which can degrade the performance.

Saha *et al.* [7] compared the performance of a single-, two-, and three-stage rotor and concluded that a two-stage turbine provides the highest power coefficient. In contrast, Jian *et al.* [13] found that the C_p of a single stage was 20% higher than a two-stage rotor, noting that the AR of the two rotors was different. Therefore, in this study, a single-stage S-rotor was chosen to be studied and enhanced by choosing the best overlap ratio and number of blades for a fixed aspect ratio.

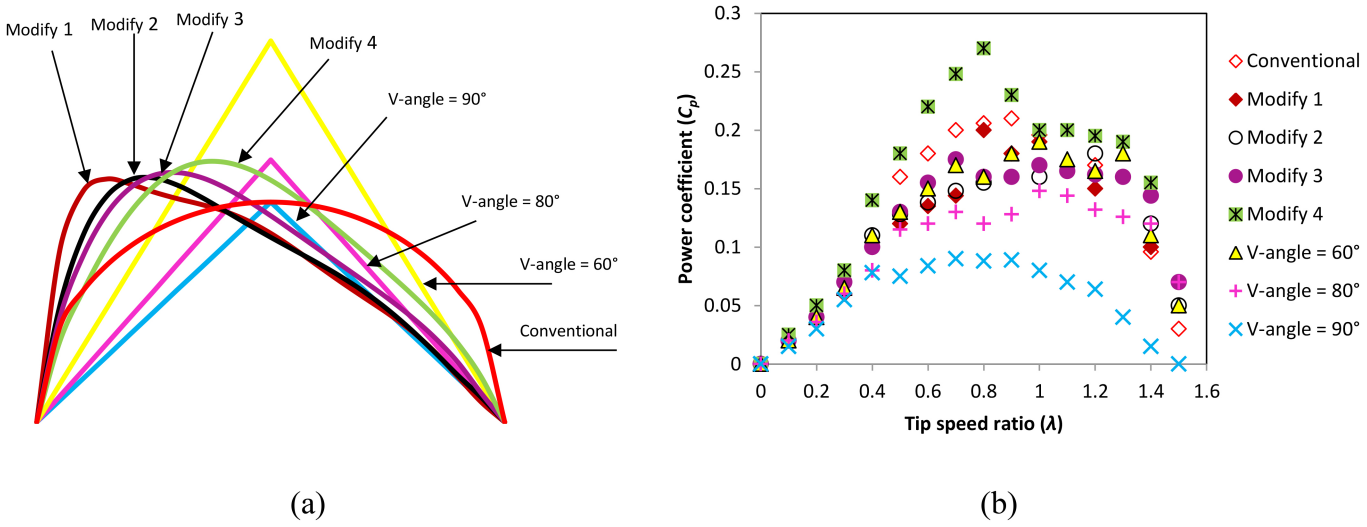

Figure 4. (a) Different blade configurations and (b) their corresponding power curves [16].

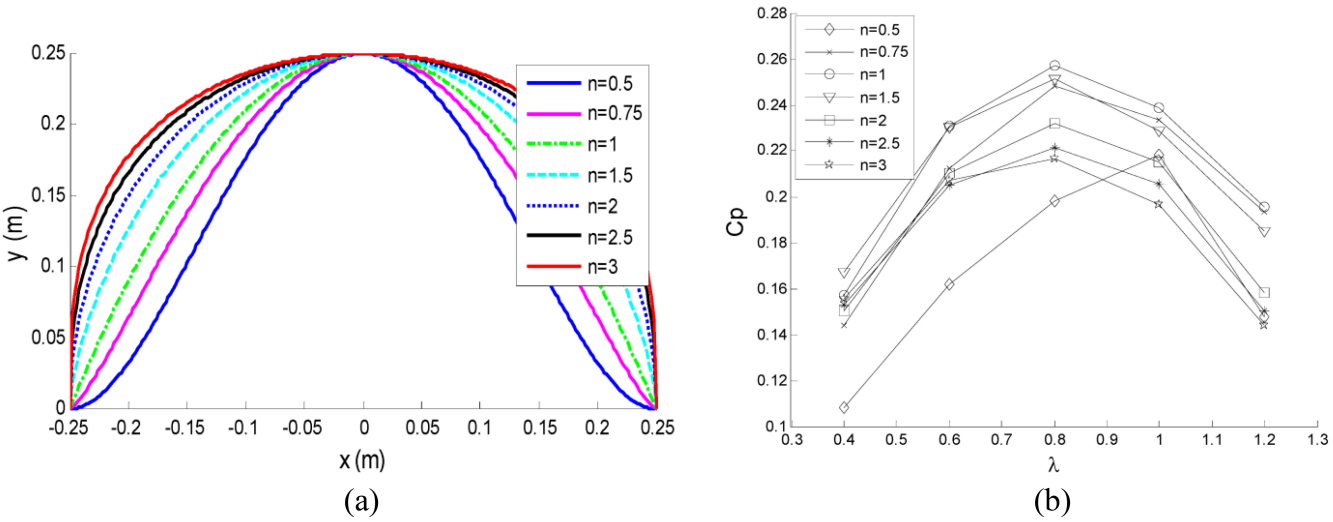

Figure 5. (a) Blade shapes with different fullness and (b) their corresponding power curves [3].

1.3 Modified Savonius: Effect of the Blade Shape

Researchers worked extensively on the optimisation of the blade shape in order to attain the maximum possible efficiency from the rotor [14], [15]. Gad *et al.* [16] studied the influence of the blade shape on the power coefficient by numerically simulating the performance of seven different rotor configurations (Figure 4(a)). The results (Figure 4(b)) showed that a new developed polynomial blade shape provides the highest power coefficient (C_p = 0.28) for a tip speed ratio of 0.8.

Similarly, Tian *et al.* [3] investigated numerically the effect of the blade fullness on the power production of the S-rotor. The author used the Myring equation $b\left[1-\frac{x^2}{a^2}\right]^{1/n}$ for the design of the blades, with a and b being constants and n varying between 0.5 and 3 (Figure 5(a)). It was found that a turbine with a blade fullness of $n = 1$ yields the highest power coefficient (C_p = 0.2573) (Figure 5(b)) with an increase of about 11% from the convention S-rotor. Roy and Saha [17] compared experimentally the performance of their novel blade design, the conventional S-rotor, Benesh, modified Bach, and semi-elliptical bladed turbines. The experiment demonstrated the superiority of the novel blade rotor over the other designs. The power coefficient was improved by a minimum of 3.3% and a maximum of 34.8% when compared with the modified Bach and the conventional Savonius, respectively.

Twisting the blades to an optimum angle can also highly improve the rotor self-starting capability as well as its overall performance [18]. Saha and Rajikumar [19] carried out wind tunnel studies to showcase the potential of the Savonius rotor with twisted blades. They found that larger twist angles improve the maximum power output and the starting characteristics of the rotor at low airspeeds. The optimum twist angle was reported to be 15° with a 21% gain in performance over the conventional S-rotor. Likewise, Damak *et al.* [20] showed that the power coefficient of a helical Savonius turbine with a twist of 180° is 20% higher than the conventional Savonius.

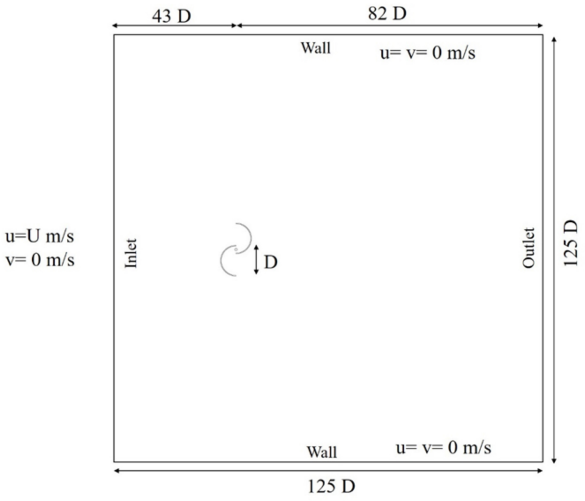

Figure 6. Computational domain with boundary conditions and dimensions.

It is clear that several attempts have been done to increase the efficiency of the Savonius wind turbine, either by changing the number of blades and number of stages or by adjusting the blade shape and varying the blade's twisting angle. In this paper, the traditional Savonius rotor will be studied by varying other parameters to enhance its performance.

2. Numerical Modelling

Numerical simulations can be conducted in two-dimensional (2D) or three-dimensional (3D) configurations. Although 2D models neglect 3D effects, previous experience shows that they can provide acceptable and indicative results in many cases [3], [12], [16], [21], [22]. In this paper, a preliminary 3D simulation is conducted using ANSYS-Fluent on a Savonius turbine in order to quantify 3D effects. In this regard, two configurations are considered: with and without endplates. Then, 2D simulations are conducted and a good agreement is obtained with the 3D model with endplates. Consequently, all remaining case studies are carried out using the 2D model to reduce the computational cost and time.

2.1 Computational Domain and Boundary Conditions

In order to simulate the behaviour of the Savonius wind turbine prototype, a 2D projection of the S-rotor, with the exact dimensions of the prototype, was inserted into a quadrilateral domain representing the wind tunnel apparatus chamber. The simulations were chosen to be steady for two reasons. On the one hand, experiments are conducted in a wind tunnel providing a steady airflow. On the other hand, transient simulations are computationally costly in terms of resources and time. For steady 2D simulations, one stationary computational domain is enough to simulate the performance of the S-rotor at a pre-fixed position. The computational domain is presented in (Figure 6).The

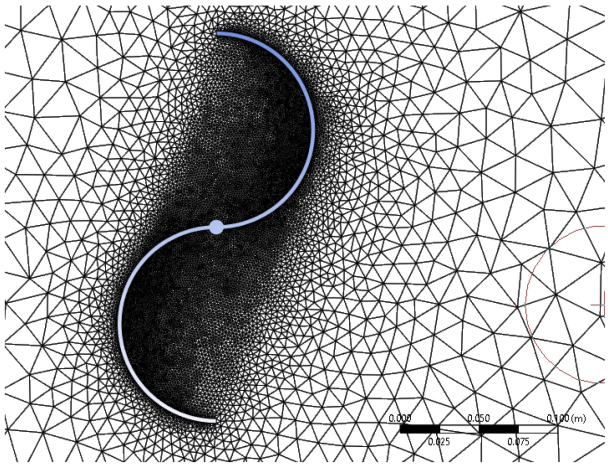

Figure 7. Mesh topology around the S-rotor.

upstream edge where the air is blown is noted as Inlet and the downstream edge at the flow exit is noted as Outlet with pressure outlet type. The lateral boundaries are stationary non-slip walls. The blade diameter is set to $D = 120$ mm and the shaft diameter is $d_{\text{shaft}} = 10$ mm.

The governing equations in a 2D system are solved to provide results for several parameters, such as pressure, moment, and velocity. These equations are the continuity (1) and the Navier–Stokes (momentum) equations (2) and (3):

$$\text{Continuity:} \quad \frac{\partial u}{\partial x} + \frac{\partial v}{\partial y} = 0 \tag{1}$$

$$x\text{-momentum:} \quad \rho\left(u\frac{\partial u}{\partial x} + v\frac{\partial u}{\partial y}\right) = -\frac{\partial p}{\partial x} + \mu\left(\frac{\partial^2 u}{\partial x^2} + \frac{\partial^2 u}{\partial y^2}\right) \tag{2}$$

$$y\text{-momentum:} \quad \rho\left(u\frac{\partial v}{\partial x} + v\frac{\partial v}{\partial y}\right) = -\frac{\partial p}{\partial y} + \mu\left(\frac{\partial^2 v}{\partial x^2} + \frac{\partial^2 v}{\partial y^2}\right) \tag{3}$$

2.2 Mesh and Grid Independence Study

The 2D S-rotor configuration is a simple geometry that makes the mesh generation process easier to handle. In this case, both structured and unstructured meshes work [23]. Nevertheless, it is important to have enough elements to capture the flow physics at the proximity of the rotor. Herein, the type of mesh used is triangular dominant as it results in faster computational simulations without affecting the accuracy of the results. The mesh was refined at the vicinity of the rotor blades by means of the edge sizing which is set to 600 divisions. The resulting domain comprises a total of 61,700 elements. The y^+ value ranges between 1 and 3 on the surface of the turbine blade. The mesh topology is shown in Fig. 7.

To ensure that the acquired results are independent of the mesh size, a mesh sensitivity study was conducted. The results are considered mesh independent once the difference in the value of the net moment (the main quantity of interest in this study) becomes negligible while continuously increasing the number of divisions per face. It is evident from Fig. 8 that the behaviour becomes asymptotic starting from 600 divisions per face. Refining the mesh further will only increase the computational

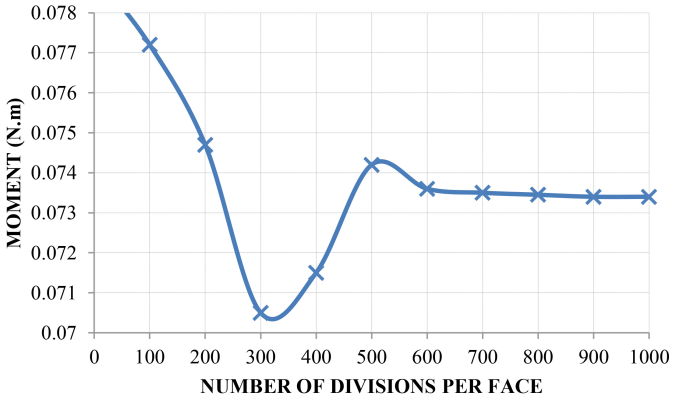

Figure 8. Mesh grid independency study.

Table 1
Air Properties

Density	Dynamic Viscosity	Kinematic Viscosity
1.225 kg/m^3	1.802×10^{-5} kg/m-s	1.470×10^{-5} m^2/s

expenses while yielding the same results. Coarsening the mesh on the other hand will lead to inaccurate results.

2.3 Turbulence Model, Convergence Criteria, and Model Inputs

Wind turbines are constantly exposed to turbulent atmospheric flow. Hence, the right turbulence model must be used in order to get a near physical representation of flow around the rotor. For these types of simulations, k–ε and k–ω are suitable models [23]. The k–ε model is widely used in numerical simulation as it is easier to implement, less time consuming than the k–ω model. The latter performs better in the case of high-pressure gradients, low Reynolds numbers, and complex and separated flows. In this study, large Reynolds number and assumingly low-pressure gradients are treated, therefore, the standard k–ε is the most suitable turbulence model [24]. For all the 2D cases, the residuals are set to 10^{-6} for both transport equations (k and ε) and similarly for the continuity, x, and y velocities. Additionally, to further ensure that the solution has converged, the drag coefficient over the blades is monitored to assure that its value becomes constant, and it is not fluctuating with each iteration.

The enclosure size is 1.5 m $\times$ 0.22 m and air at 15 °C is the working fluid whose properties are listed in Table 1. Different turbine models were simulated, and their reference data are listed in Table 2.

3. Results

3.1 3D Model

Preliminary 3D simulations were achieved to determine the effect of endplates on the output torque. The models with and without endplates delivered torques of 0.034 N.m and 0.022 N.m, respectively, showing an increase of 55%. Pressure contours (Figure 9) show that adding endplates renders a more uniform distribution in the axial direction, thus reducing 3D effects. Therefore, 2D results (presented hereafter) are in accordance with the 3D model with endplates. Henceforward, to determine other optimum parameters, subsequent simulations are conducted on 2D models.

Table 2
Reference Data versus Overlap Ratio

Overlap Ratio	Diameter (m)	Area (m^2)	Reynolds Number for $V = 7$ m/s
0%	0.1200	0.026400	57103
15%	0.1020	0.022440	48537
16%	0.1008	0.022176	47967
17%	0.0996	0.021912	47395
18%	0.0984	0.021648	46825
19%	0.0972	0.021384	46254
20%	0.0960	0.021120	45683
22%	0.0936	0.020592	44541
25%	0.0900	0.019800	42827

3.2 2D Pressure Distributions

The pressure difference between the front and rear areas of the conventional S-rotor is presented in Fig. 10(a) in order to quantify the effect of each region of the blades on the overall performance of the turbine. It can be noticed that the pressure is uniform at the upstream and downstream of the upper blade (advancing blade). The constant pressure at the upper blade generates a drag force, subsequently, a torque that rotates the turbine about the shaft in the clockwise direction. On the other hand, only a small part of the lower blade (returning blade) is positively contributing to the net torque. A big portion of the lower blade, marked with a dashed rectangle in Fig. 10(b), is actually generating a counter torque. This is due to the fact that in this region, the pressure upstream is higher than the pressure downstream.

3.3 Overlap Ratio

Overlapping the blades up to a certain extent can significantly reduce the ineffective part of the lower blade. Accordingly, simulations of several overlap ratios ranging between 0% and 25% are conducted at inlet speeds of 3, 5, and 7 m/s. The net torque generated by the turbine at each overlap ratio and various inlet speeds is acquired at an angle of 0° is shown in Table 3.

The net torque obtained corresponds to the turbine at a specific orientation with respect to the direction of the wind. Because the torque values are very close at this

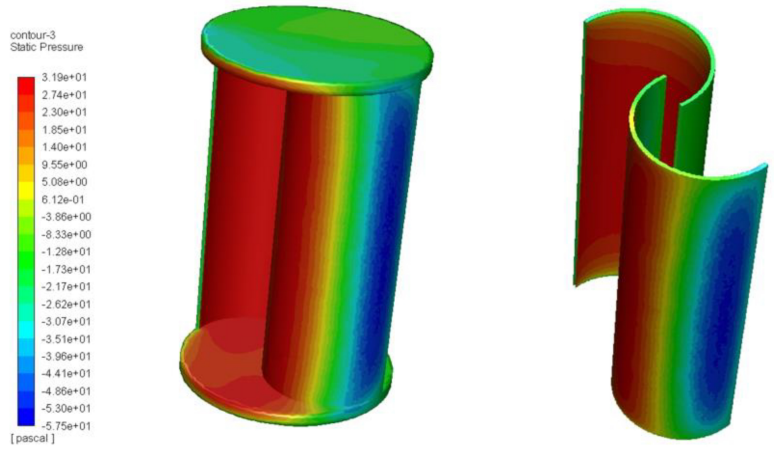

Figure 9. Pressure contours for 3D models with endplates (left), and without endplates (right).

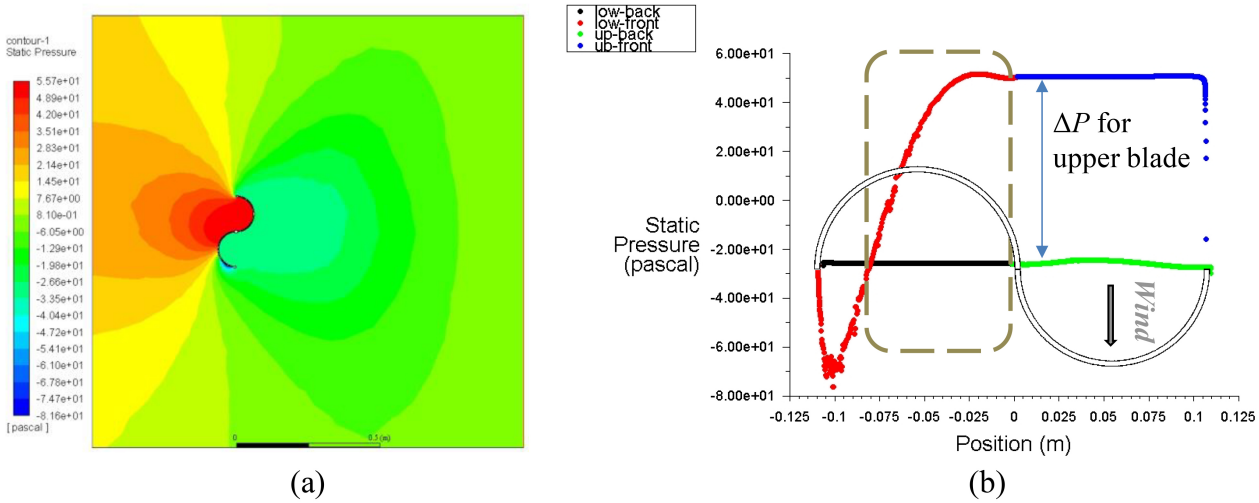

(a) (b)

Figure 10. (a) Pressure contours about the conventional Savonius rotor and (b) the corresponding pressure plot at the upstream and downstream area of the blades.

angle, no clear deduction can be made. Hence, additional simulations at different angles of rotation are performed to obtain more representative value of the turbine's output. In each simulation, the turbine is rotated by an increment of 15° until a full revolution is achieved. The variation of the torque at each angle for three different rotor configurations (*i.e.*, 0%, 18%, and 24% overlap ratio) are plotted with the correspondent average torque for one full revolution (Figure 11). It is obvious that both the 18% and 24% overlap ratios rendered much significant average torque values for one full revolution compared to the configuration with no overlap.

4. Experimental Validation

In order to validate the previously obtained numerical results, an experimental prototype was tested in a PLINT TE-54 subsonic wind tunnel (Figure 12). A 5-inch PVC pipe was cut longitudinally in half to obtain two semi-cylinders. Two 2-mm thick wooden disks with a diameter of 12 cm from the endplates inside which the S-shape of the rotor was carved. The main reason for adopting a prototype with endplates is the good agreement in numerical results between the 2D model and the 3D model with endplates. A tachometer was used to measure the free rotational speed of the turbine, *i.e.*, when it is subjected to zero load. The wind speed was measured with the help of a digital hot wire anemometer.

The overlap ratio was varied using an adjustable mechanism while maintaining the same blade size. Hence, this resulted in a decrease of the turbine outer diameter with increasing overlap ratio. A total of four different overlap ratios were tested: 0%, 24%, 40%, and 80%. Consequently, the results (Figure 13) show the combined effect of overlap ratio and turbine outer diameter on the rotational speed. On the one hand, increasing the overlap ratio up to 40% tends to increase the rotational speed, while further increase in overlap ratio (80%) would result in a decrease in rotational speed. On the other hand, decreasing the turbine outer diameter would result in a decrease of the output torque despite the increase in rotational speed. This could be explained by the appearance of vortices in the overlap space, especially in the case of relatively high overlap ratios.

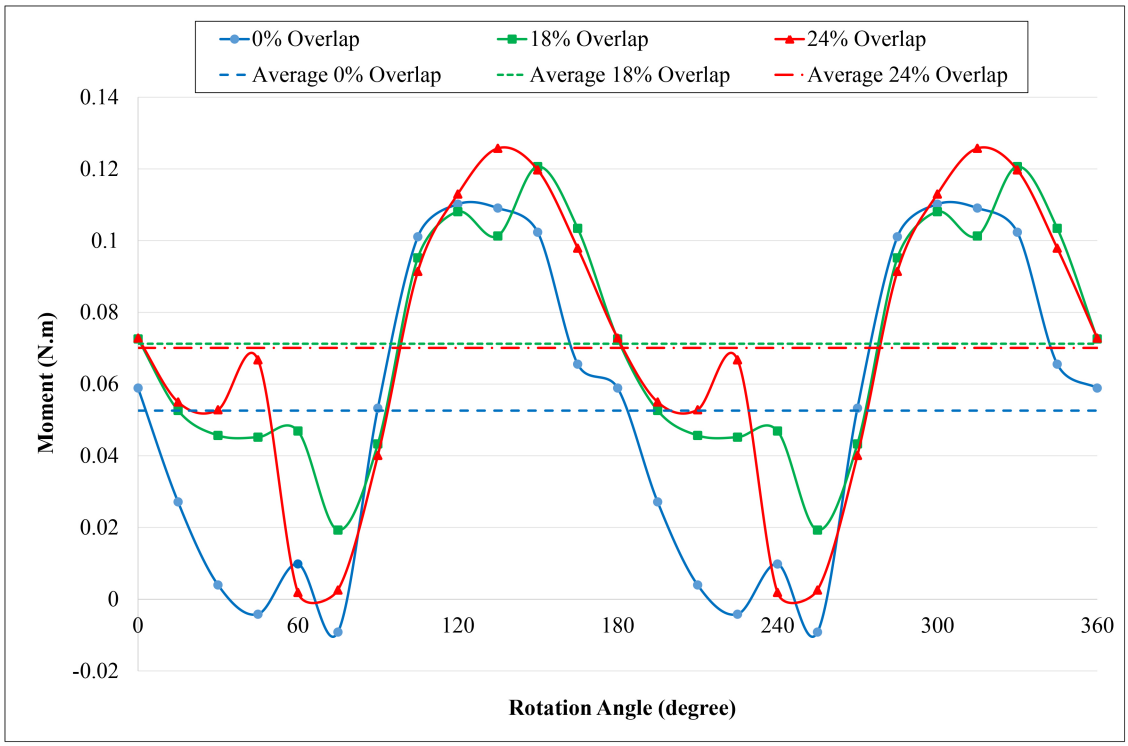

Figure 11. Net torque at various angles for one full rotation at 7 m/s wind velocity.

Table 3
Net Torque Output at Different Overlap Ratios and Various Inlet Speeds

	Wind Velocity		
	3 m/s	5 m/s	7 m/s
Overlap Ratio	**Net Torque Output (N.mm)**		
0%	12.7	36.5	71.6
15%	11.9	35.2	71.0
16%	12.6	36.7	73.0
17%	12.3	35.9	72.5
18%	12.6	36.7	73.2
19%	12.8	36.7	72.7
20%	12.8	36.7	73.0
22%	12.7	36.8	72.9
25%	12.5	36.0	71.6

It is obvious that reaching 80% overlap ratio is not efficient at all where vortices and negative drag will increase drastically leading to slower rotational speeds. Although a 40% overlap ratio yielded the highest rotational speed, the turbine exhibited severe vibrations due to vortices in the overlap space. Moreover, a 24% overlap ratio rendered very close RPM values compared to the 40% and better ones compared to no overlap (0%) but with minor vibrations worth mentioning.

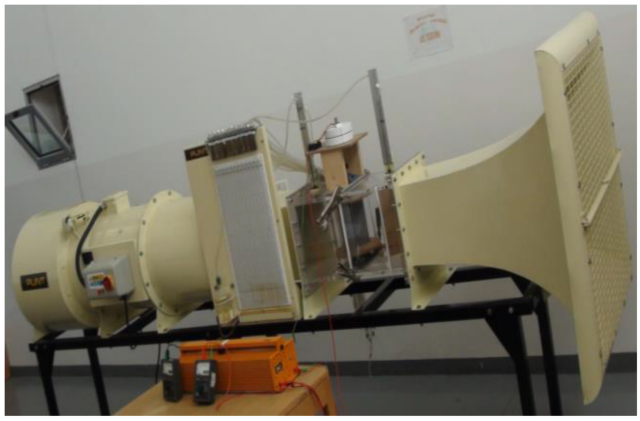

Figure 12. Wind tunnel testing setup.

Based on both numerical and experimental results, it was found that a two-bladed Savonious wind turbine would produce the best performance for an overlap ratio ranging between 15% and 25%. The main drawbacks of further increase in overlap ratio are a lower expected output power (because of decreased outer diameter and output torque) and amplified vibrations (possibly because of stronger vortices in overlap space).

5. Conclusion

This work assessed the design parameters of a two-bladed Savonius wind turbine with particular focus on the effect of the overlap ratio on the turbine performance. In this context, numerous CFD models were tested in 2D and 3D simulations. Then, experimental measurements were

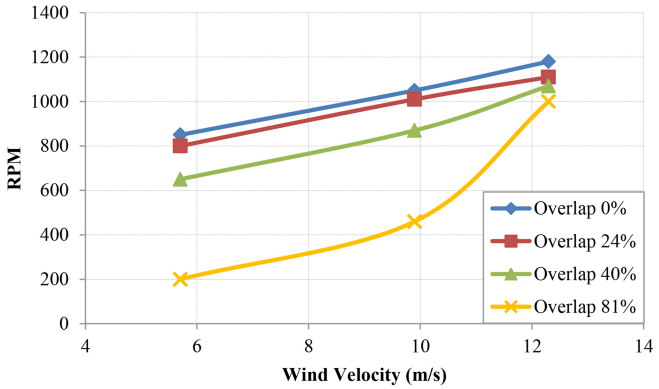

Figure 13. Experimental results of RPM variations versus wind speed.

conducted in a wind tunnel in order to validate numerical outcomes.

It was found that adding endplates to the turbine will significantly improve its performance. The endplates reduce the tip vortices effects resulting in a more uniform pressure distribution in the axial direction. In addition, a 2D numerical model simulated with good agreement a 3D model with endplates.

Concerning the overlap ratio, numerical results showed an increase in the output torque compared to the conventional configuration (no overlap). However, the best results were obtained in the range of 15%–25% overlap. Beyond this range, higher rotational speeds may be obtained coupled with severe vibrations leading to a degradation in output power.

Further recommendations include a numerical study with a dynamic mesh which allows obtaining more realistic results as the output torque would be determined for a full rotation of the turbine. Moreover, experimental testing could be carried out with a variable applied load on the turbine which allows determining the turbine output power. Finally, additional modification on the blade design could be implemented (modifying blade shape, covering the counter blade, adding fins on the backside of the blades, *etc.*).

Acknowledgement

This work was supported by the Lebanese Council of Scientific Research (CNRS-L) under Grant number 02-02-18.

References

[1] R. Alayi, M. Jahangiri, J.W.G. Guerrero, R. Akhmadeev, R.A. Shichiyakh, and S.A. Zanghaneh, Modelling and reviewing the reliability and multi-objective optimization of wind-turbine system and photovoltaic panel with intelligent algorithms, *Clean Energy*, *5*(4), 2021, 713–730.

[2] A. Masih and H.K. Verma, Optimization and reliability evaluation of hybrid solar-wind energy systems for remote areas, *International Journal of Renewable Energy Research*, *10*(4), 2020, 1697–1706.

[3] W. Tian, B. Song, J.H. van Zwieten, and P. Pyakurel, Computational fluid dynamics prediction of a modified Savonius wind turbine with novel blade shapes, *Energies*, *8*(8), 2015, 7915–7929.

[4] H.H. Al-Kayiem, B.A. Bhayo, and M. Assadi, Comparative critique on the design parameters and their effect on the performance of S-rotors, *Renewable Energy*, *99*, 2016, 1306–1317.

[5] R.E. Sheldahl, B.F. Blackwell, and L.V. Feltz, Wind tunnel performance data for two-and three-bucket Savonius rotors, *Journal of Energy*, *2*(3), 1978, 160–164.

[6] M.H. Ali, Experimental comparison study for Savonius wind turbine of two & three blades at low wind speed, *International Journal of Modern Engineering Research*, *3*(5), 2013, 2978–2986.

[7] U.K. Saha, S. Thotla, and D. Maity, Optimum design configuration of Savonius rotor through wind tunnel experiments, *Journal of Wind Engineering and Industrial Aerodynamics*, *96*(8–9), 2008, 1359–1375.

[8] M. Zemamou, M. Aggour, and A. Toumi, Review of Savonius wind turbine design and performance, *Energy Procedia*, *141*, 2017, 383–388.

[9] M.A. Kamoji, S.B. Kedare, and S.V. Prabhu, Experimental investigations on single stage modified Savonius rotor, *Applied Energy*, *86*(7–8), 2009, 1064–1073.

[10] N. Fujisawa, On the torque mechanism of Savonius rotors, *Journal of Wind Engineering and Industrial Aerodynamics*, *40*(3), *1992*, 277–292.

[11] B.F. Blackwell, L.V. Feltz, and R.E. Sheldahl, *Wind tunnel performance data for two-and three-bucket Savonius rotors.* (Springfield, VA: Sandia Laboratories, 1977), 1–105.

[12] J.L. Menet and N. Bourabaa, Increase in the Savonius rotors efficiency *via* a parametric investigation, *Proc. European Wind Energy Conf. & Exhibition*, London, Nov. 2004, 22–25.

[13] C. Jian, J. Kumbernuss, Z. Linhua, L. Lin, and Y. Hongxing, Influence of phase-shift and overlap ratio on Savonius wind turbine's performance, *Journal of Solar Energy Engineering*, *134*(1), 2012, 1–9.

[14] W.A. El-Askary, A.S. Saad, A.M. Abdel Salam, and I.M. Sakr, Experimental and theoretical studies for improving the performance of a modified shape Savonius wind turbine, *Journal of Energy Resources Technology*, *142*(12), 2020, 121303.

[15] Z. Mu, G. Tong, Z. Xiao, Q. Deng, F. Feng, Y. Li, and G.V. Arne, Study on aerodynamic characteristics of a Savonius wind turbine with a modified blade, *Energies*, *15*, 2022, 6661.

[16] H.E. Gad, A.A. Abd El-Hamid, W.A. El-Askary, and M.H. Nasef, A new design of Savonius wind turbine: Numerical study, *CFD Letters*, *6*(4), 2014, 144–158.

[17] S. Roy and U.K. Saha, Wind tunnel experiments of a newly developed two-bladed Savonius-style wind turbine, *Applied Energy*, *137*, 2015, 117–125.

[18] A.S. Saad, I.I. El-Sharkawy, S. Ookawara, and M. Ahmed, Performance enhancement of twisted-bladed Savonius vertical axis wind turbines, *Energy Conversion and Management*, *209*, 2020, 112673.

[19] U.K. Saha and M.J. Rajkumar, On the performance analysis of Savonius rotor with twisted blades, *Renewable Energy*, *31*(11), 2006, 1776–1788.

[20] A. Damak, Z. Driss, and M.S. Abid, Experimental investigation of helical Savonius rotor with a twist of 180°, *Renewable Energy*, *52*, 2013, 136–142.

[21] M.H. Mohamed, G. Janiga, E. Pap, and D. Thévenin, Optimization of Savonius turbines using an obstacle shielding the returning blade, *Renewable Energy*, *35*(11), 2010, 2618–2626.

[22] W.A. El-Askary, M.H. Nasef, A.A. Abdel-Hamid, and H.E. Gad, Harvesting wind energy for improving performance of Savonius rotor, *Journal of Wind Engineering and Industrial Aerodynamics*, *139*, 2015, 8–15.

[23] *Fluent thoery guide*, (Canonsburg, PA: ANSYS Inc., 2013).

[24] F.R. Menter, Two-equation eddy-viscosity turbulence models for engineering applications, *AIAA Journal*, *32*(8), 1994, 1598–1605.

Biographies

Zaki Alomar received the MSc. degree in mechanical engineering from the University of Balamand in 2018. He worked as a Research Assistant with the University of Balamand on the vertical axis wind turbine project with the aim to improve its efficiency. He is currently pursuing the Ph.D. degree in advanced systems engineering with the Free University of Bolzano/Bozen, Italy. His work involves the design, modelling, simulation, and application of additively manufactured metallic lattice structures.

Gerard Khoury currently works with Dar Al-Handasah (Shair & Partners) in the Mechanical & Industrial Design Unit as a Plant Design Engineer. He received the master's degree in mechanical engineering (Thermofluids) from the University of Balamand. He does research in mechanical engineering, multiphase flow, and vertical axis wind turbines.

Jihad Rishmany was born in Lebanon in 1979. He received a Mechanical Engineering Diploma from the Lebanese University in 2002, and the Ph.D. degree from ENSICA, France, in 2007. He did a postdoctoral research in tribology with Ecole Des Mines in Albi, France, in 2008. In 2009, he joined the University of Balamand, Lebanon, where he is currently an Associate Professor with the Mechanical Engineering Department. He has taught more than 20 different courses at both undergraduate and graduate levels. His main research areas include renewable energy, finite-element analysis, multibody dynamics, waste management, and waste-to-energy.

Michel Daaboul was born in Lebanon, in 1982. He received the Mechanical Engineering degree from the Lebanese University, Beirut, Lebanon, in 2005, and the master's degree in fluid mechanics and aerodynamics and the Ph.D. degree in fluid mechanics from the University of Poitiers, France, in 2006 and 2009, respectively. He is currently an Associate Professor with the University of Balamand, Lebanon, where he joined the Mechanical Engineering Department in 2010. He teaches fluid mechanics, aerodynamics, heat transfer, thermodynamics, turbomachinery, and propulsion. His research works focus on renewable energy as well as on developing EHD actuators for flow control and liquid atomization.